

# APPLICATION OF WIWEDEMEN- FRANZE –LORANZE LAW TO INVESTIGATE THE EFFECT OF TEMPERATURE AND SECTION THICKNESS ON THE THERMAL CONDUCTIVITY OF DUCTILE GRAPHITE CAST IRON

Omar Elmabrouk

Department of Industrial and Manufacturing System Engineering,  
Garyounis University, Benghazi, Libya

## ABSTRACT

A direct resistance measurement method using two point probes has been used to measure the electrical resistance of ductile graphite cast iron produced at different thickness sections and over a wide range of temperatures. The thermal conductivity of this type of cast iron was estimated using the Wiwedemen- Franze –Loranze Law. It was found that smaller section thickness has lower thermal conductivity than medium and larger thicknesses. This is due to the formation of compacted and degenerated ductile cast iron at higher section thicknesses.

في هذا البحث تم تطبيق طريقه العالم فرانز لورانز لحساب التوصيل الحراري لمعدن الحديد الزهر الكروي عندما ينتج في مقاطع ذات اسماك مختلفة و عند درجات حرارة عاليه. حيث تم قياس المقاومة الكهربائية مباشرة من خلال الاتصال المباشر عند نقطتين لعينات من المعدن، ووجد أن التوصيل الحراري لهذا المعدن يزداد عند ينتج هذا النوع من الحديد الزهر في المقاطع السمكة ويقل التوصيل الحراري عندما ينتج هذا النوع من الحديد الزهر في المقاطع المتوسطة و الصغيرة و السبب في ذلك ناتج عن تكون حديد زهر مضغوط وحديد زهر كروي متشجر في هذه المقاطع.

**Keywords:** Electrical resistance, thermal conductivity, ductile graphite iron.

## 1. INTRODUCTION

In some applications, such as cylinder heads, pistons, and brake drums, thermal conductivity is the main reason for the material selections. Cast irons have been used in such applications, since it combine good mechanical and friction property as well as a good thermal conductivity [1].

The thermal conductivity of all cast iron appears to be controlled by the form, amount, and distribution of graphite [2]. Because of the different interconnected network of the graphite particles in compacted graphite iron, its thermal conductivity is only slightly lower than that of grey iron, but much higher than that of ductile iron [3]. Thermal conductivity values of metallographic phases of cast iron are presented in Table 1. It can be seen that ferrite has higher thermal conductivity than pearlite and also that cementite can lower the cast iron thermal conductivity. [4]. Typical values of thermal conductivity of different gray and ductile iron grades are presented Tables 2 and 3 for evaluated temperatures. For grey irons, thermal conductivity decreases with temperature. This trend is observed in many reports [5, 6, 7, 8], although there is no discussion on the cause of this behavior.

Relatively, few studies have been reported on the electrical conductivity at elevated temperature, since the measurements are extremely difficult, and it's difficult to measure thermal conductivity of metals

and alloys precisely. In this paper we present the results of electrical conductivity of ductile compacted and flake cast iron and estimate the thermal conductivity of these types of cast iron over a wide range of temperatures.

## 2. EXPERIMENTAL PROCEDURE

### 2.1 Material and Processing

Ductile irons was produced in a step block casting in green sand with 5, 10, 20, 40, mm thick steps as illustrated in Fig. 1. Sorel white cast iron and steel scrap were used as basic charge material. FeSiMg-Cermish metal used as an agent material, Cu and, FeSi were used as an alloying element, 0.5% FeSi was used as post inoculation. The chemical composition of these materials is shown in Table 4.

### 2.2 Melting Procedure

Once the charge materials, Sorel and Steel scrap, prepared and calculated, they were melted down using a 10-17 kg capacity induction furnace installed with a clay graphite crucible. After having molten metal, alloying materials such as Cu, and FeSi were added to the molten charge. In the stage of spheroidizing treatment, FeSiMgCerium Misch metal was added by plunging method with the plunger ladle shown in Fig. 2. The treatment temperature varied in the range of 1425 to 1475 °C. Post inoculation was accomplished by adding 75% foundry grade ferrosilicon (lump size are in between 1-2 mm) from

the top of the molten metal in the ladle. The molten metal was stirred to ensure complete solution and reaction inoculation. The treatment time and post inoculation time were 5 to 7 minute and 1.5 minute respectively. The pouring temperatures were in the range of 1400 to 1420 °C. In order to understand the specimen belongs to which section thicknesses, codes were given to the samples. The sample codes are shown in Table 5.

### 2.3 Sample Preparation and Optical Microscopy Studies

The metallographic specimen was cut from each section of the stepped block. Specimens were prepared by using abrasive emery papers and were polished on METASERV universal polisher Equipment. The specimens were machined to the dimension shown in Fig. 3 and examined by optical microscope. The microphotographs were taken by NIKON OPTIPHOT.

### 2.4 Electrical and Thermal Conductivity

The variation of thermal conductivity of each specimen with temperatures gradient ranging from room temperatures to 500 °C was found via measuring electrical resistance.

The two point probe measurement technique shown in Fig. 4 was used for high temperature measurements.

The used set up is similar to the one used by M.Ali AKBAŞ [10], but, in this set up instead of using Nano voltmeter the digital voltmeter is equipped .This sep up consists of 30 cm long and 1.2 cm in dimeter alumia tube with closed bottom as the main part. Figure 5 shows the scheme of the specimen fixing mechanism used in high temperature resistivity measurements. In this tube there is window close to the bottom which used for changing the specimen.An alumina spaghetti in bottom of the tube was fixed by an alumina cement .Another spaghetti which was able to move up and down was attached to the open end by using a special mechanism made from brass.

The samples to be measured were placed between these two sapghtties and a pressure was applied to get better contacts.Utilizing this mechanism ,it was possible to measure resistance of specimens simply by pumping 1 A constant current throught the Pt-Pt/13% Rh wires and detecting the potential drop in the specimen by means of Pt wires.

**Table 1**, Thermal conductivity of main metallographic phases of cast irons at room temperature [8]

Metallographic constituent	Thermal conductivity, W m-1 °C-1		
	0 – 100 °C	500 °C	1000 °C
Ferrite	71 – 80	42	29
Pearlite	50	44	40
Cementite	7 – 8	-	-
Graphite	-	-	-
Parallel to basal plane	293 - 419	84 – 126	42 – 63
Perpendicular to basal plane	84	-	-

**Table 2**, Results of thermal conductivity for different grades of gray Iron [7]

Temperature (C)	Thermal conductivity (W/K.m)					
	GJL 150	GJL 200	GJL 250	GJL 300	GJL 350	GJL 400
100	52,5	50,8	48,8	47,4	45,7	44,0
200	51,5	49,8	47,8	46,4	44,7	43,0
300	50,5	48,8	46,8	45,4	43,7	42,0
400	49,5	47,8	45,8	44,4	42,7	41,0
500	48,5	46,8	44,8	43,4	41,7	40,0

**Table 3** Results of thermal conductivity for ductile irons [9]

	GGG-35.3	GGG-40	GGG-50	GGG-60	GGG-70	4 Si-Mo
100 °C	40.2	38.5	36.0	32.9	29.8	25.1
200 °C	43.3	41.5	38.8	35.4	32.0	27.2
300 °C	41.5	39.8	37.4	34.2	31.0	28.1
400 °C	38.8	37.4	35.3	32.8	30.3	28.6
500 °C	36.0	35.0	33.5	31.6	29.8	28.9

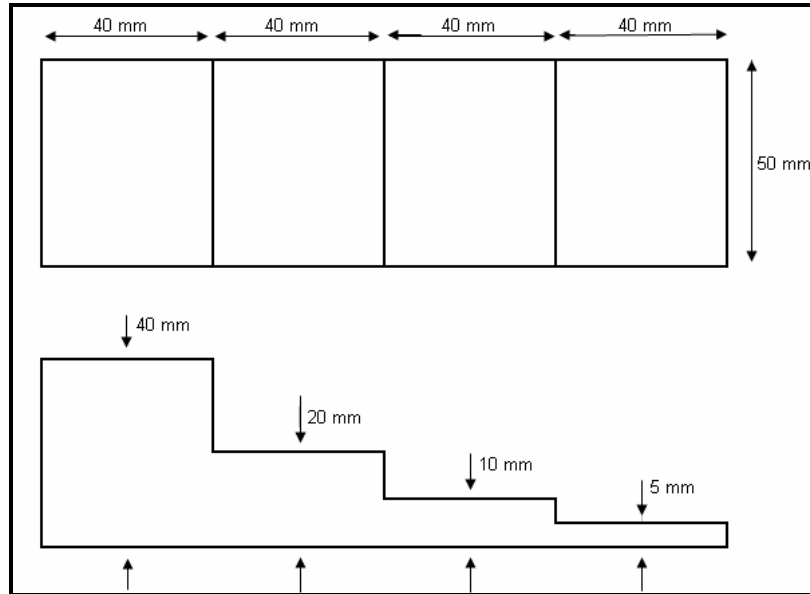


**Fig.1** Step block with 5, 10, 20 and 40 mm thick steps

**Table 4,** Chemical composition of charge material.

Charge Material	%C	%Si	%Mg	%Ca	%Al	%RE	%V	%S	%P	%Cu	%Fe
Sorel white cast iron	4,3	0,2					0,2	0,02	0,02		Blance
Steel	0,2	0,2					0,3	0,02	0,07		Blance
Scrap											
FeSiMgCe		44-48	5,5-6,5	0,2-0,6	Max 1,2	2,5					Blance
Misch metal											
FeSi		75		0,8							Blance
Cu										Pure	
Post		75									Blance
Inoculation											

**Table 5** Descriptions of Cods

Code	Descriptions
1	Mg/S ratio 6.5
A	Trail made by using FeSiMg-Cermish metal
d	5 mm section thickness
e	10 mm section thickness
f	20 mm section thickness
g	40 mm section thickness

Example: 1 Ag is a sample taken from 40 mm section thickness of the heat of FeSiMg- Cermish metal treatments in which the ratio of Mg/S is 6.5.

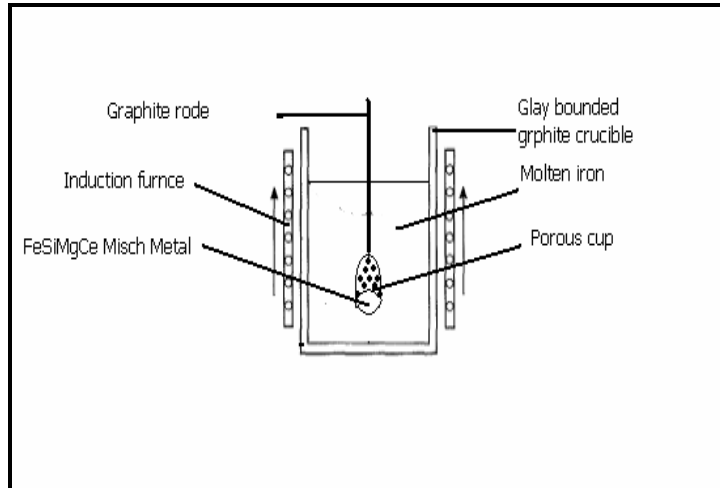


Fig. 2 Plunger Ladle Techniques

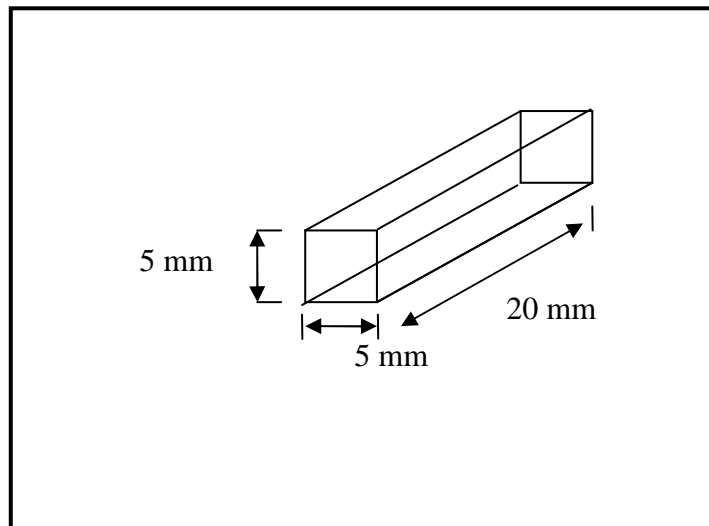


Fig. 3 Electrical resistivity specimen

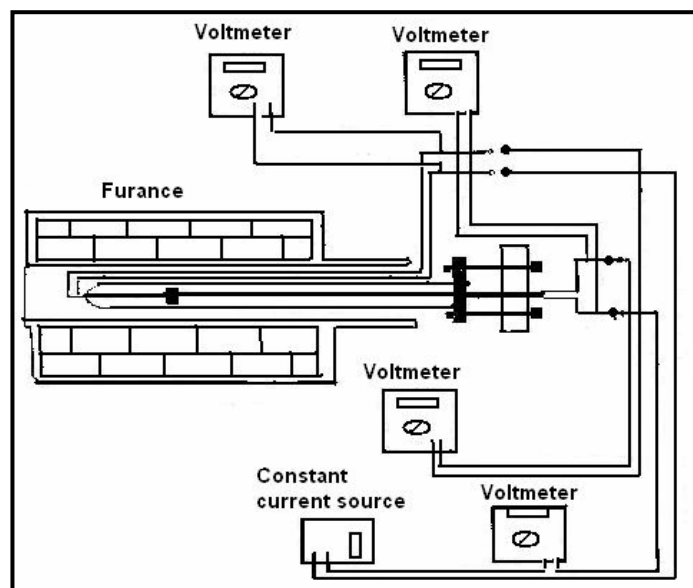
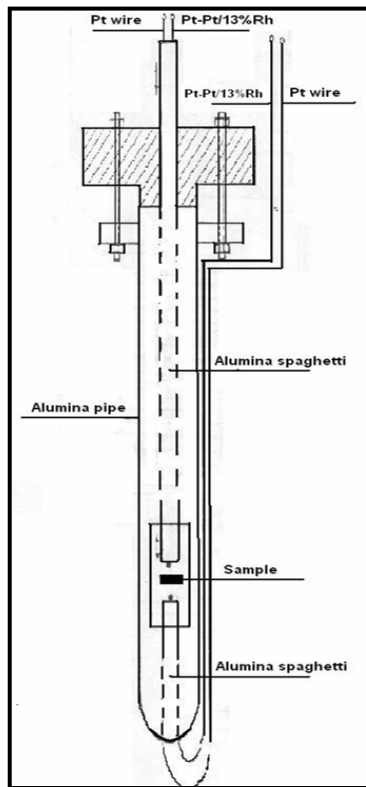


Fig. 4 The setup used for electrical resistance measurements [3]



**Fig. 5** The scheme of the specimen fixing mechanism used in high temperature resistance measurements [3]

As it's well known, the free electrons are primarily responsible for the electrical and thermal conductivity of metals and alloys; therefore, the Wiedemann-Franz-Loranz Law can be applied to relate the thermal conductivity to the electrical resistivity as follows.

$$\frac{\lambda \rho_e}{T} = \frac{\pi^2 K^2}{3 e^2} = L_0$$

Where  $\lambda$  is the thermal conductivity, T is the absolute temperature.  $\rho_e$  is the electrical resistivity, K is the Boltzman constant and e is the electron charge

The constant

$$L_0 = \frac{\pi^2 K^2}{3 e^2} = 2.445 \times 10^{-8} \text{ w}\Omega K^{-2}$$

The electrical resistance (R) and electrical resistivity ( $\rho_e$ ) are

$$R = \frac{\rho_e L}{A}$$

Where L and A are the length and the cross-section area of specimen Therefore,

$$\lambda = \frac{2.445 \times 10^{-8} \times T \times L}{R \times A}$$

### 3. RESULTS AND DISCUSSION

At spheroidizing potential, Mg/S ratio equal to 6.5 and with the chemical composition shown in Table 6, the graphite shape was spheroidal in the small section and spheroidal with degenerated graphite in the medium and large section. Figures 6 through 9 show the microstructures of sections varying from 5 to 40 mm. The electrical resistance of each section was measured; the results are shown in Table 7.

Figures 10 present the variation of thermal conductivity of ductile cast iron estimated by Wiedemann-Franz-Lorenz Law with temperature for 1Ad, e, f.

After presenting the results, it is seen that there is a good agreement between these results with the results from the literature; however the small variations can be attributed to the contact problem between the samples and the thermocouples. This contact is becoming week especially at high temperatures resulting in increasing the electrical resistance and then decreasing the thermal conductivity.

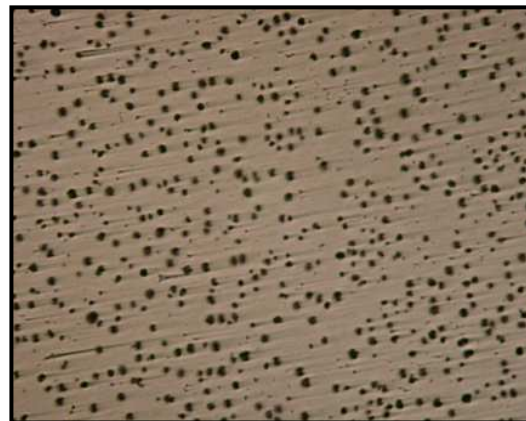


**Fig. 6** Microstructure of specimen

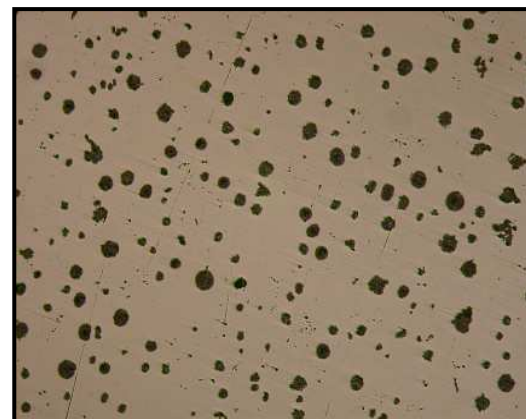


**Fig. 7** Microstructure of specimen with 1Ad code. Magnification  $\times 100$  with 1Ae code .Magnification  $\times 100$

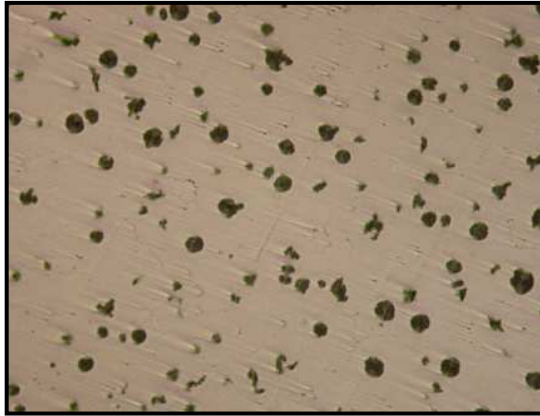


Fig. 8 Microstructure of specimen

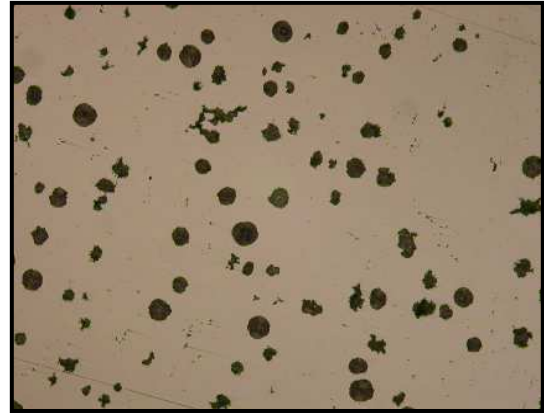


Fig. 9 Microstructure of specimen with 1Af code. Magnification  $\times 100$  with 1Ag code. Magnification  $\times 100$

Table 6 Chemical composition

%Si	%C	%Mg	%Cu	%S	%Mn	%P	%Cr	%CerMM
2.757	3.755	0.066	0.798	0.0108	0.017485	0.000886	0.00024165	0.090818363

Table 7, The Electrical Resistance of 1A heat

Temperature (K)	Resistance of 1Ad ( $\Omega$ )	Resistance of 1Ae ( $\Omega$ )	Resistance of 1Af ( $\Omega$ )	Resistance of 1Ag ( $\Omega$ )
298				
323	0,000204	0.000203	0,000201	0,000195
373	0,000234	0.000233	0,00023	0,000222
423	0,000264	0.000266	0,000257	0,000253
473	0,000294	0.000292	0,000289	0,000279
523	0,000321	0.000321	0,000316	0,000308
573	0,000355	0.000351	0,000347	0,000338
623	0,000383	0.000375	0,000377	0,000365
673	0,000414	0.00041	0,000404	0,000395
723	0,000441	0.000438	0,00043	0,000422
773	0,000467	0.000461	0,000457	0,000447

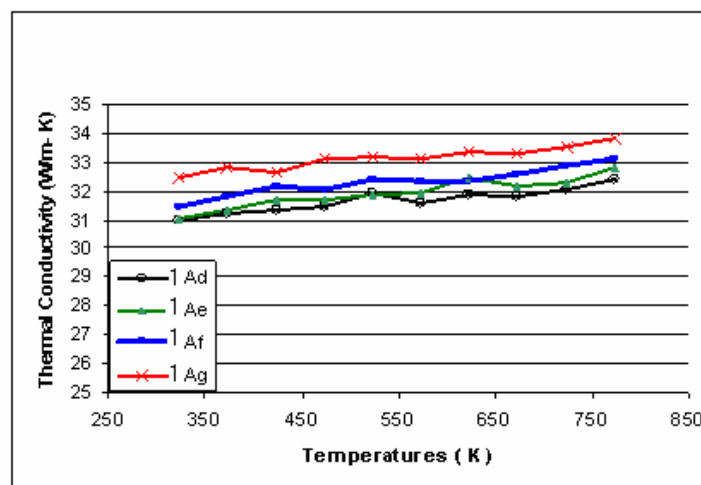


Fig. 10 Variation of thermal conductivity of 1Ad, e, f and g with temperature

#### 4. CONCLUSION

The result showed that, the ductile cast iron has highest thermal conductivity at larger thickness followed by intermediate thicknesses, smaller thicknesses exhibits the lowest thermal conductivity. This is due to the presence of compacted and degenerated graphite cast iron.

#### 5. REFERENCES

- [1] W. L. Guesser, I. Masiero, E. Melleras, C. S. Cabezas UDESC , "Thermal Conductivity of Gray Iron and Compacted Graphite Iron Used for Cylinder Heads", Revista Matéria, v. 10, n. 2, pp. 265 – 272, Junho de 2005
- [2] Gürolhan Yaşar,"Compacted / Vermicular Graphite Production Techniques and The section Sensitivity of Compacted /Vermicular Graphite." M.S thesis, METU. , 1996
- [3] James P. Hrusovsky," Factors Effecting Graphite Morphology , Matrix Structures and tensile properties of Compacted Graphite Cast Iron, Ph.D. Thesis, Case Western Reserve University, 1982
- [4] HASSE, S., Duktile Gusseisen. Schiele & Schön, Berlin, 1996.
- [5] ANGUS, H.T., "Cast Iron: Physical and Engineering Properties", BCIRA, pp. 126-134, 1960.
- [6] "Thermal Conductivity of Unalloyed Cast Iron", BCIRA Broadsheet 203, 1981.
- [7] Gusseisen mit Lamellengraphit – Eigenschaften und Anwendung. Konstruieren + Giessen, Zentrale für Gussverwendung. VDI-Verlag, Düsseldorf, 2000.
- [8] STEFANESCU, D., "Physical Properties of Cast Iron", In: GOODRICH, G.M., Iron Casting Engineering Handbook, AFS,2003
- [9] Gusseisen mit Kugelgraphit, Konstruieren + Giessen. Zentrale für Gussverwendung, VDI-Verlag, Düsseldorf, 1988.
- [10] M.Ali AKBAŞ,"Effect of Ni and Ti Substitution on the Superconducting Properties of YBa<sub>2</sub>Cu<sub>3</sub>O<sub>7-X</sub> System." M.S thesis, METU. , 1991.